Potential tools for eradicating HIV reservoirs in the brain: the development of Trojan horse prodrugs for the inhibition of P-glycoprotein with anti-HIV-1 activity

Neha Agrawal[a,‡], Jennifer Rowe[a,‡], Jie Lan[b], Qigui Yu[b], Christine A. Hrycyna[a] and Jean Chmielewski[a,*]

[a]Department of Chemistry, Purdue University, 560 Oval Drive, West Lafayette, IN 47907-2084, USA

[b]Department of Microbiology and Immunology, Indiana University School of Medicine, Indianapolis, IN 46202, USA

KEYWORDS. P-glycoprotein, HIV, antiretroviral, protease, reverse transcriptase, heterodimer, prodrug, inhibition

ABSTRACT: Combination antiretroviral therapy is the mainstay of HIV treatment, lowering plasma viral levels below detection. However, eradication of HIV is a major challenge due to cellular and anatomical viral reservoirs that are often protected from treatment by efflux transporters, such as P-glycoprotein (P-gp) at the blood-brain barrier (BBB). Herein we described a Trojan horse approach to therapeutic evasion of P-gp based on a reversibly-linked combination of HIV reverse transcriptase and protease inhibitors. Potent inhibition of P-gp efflux in cells, including human brain endothelial cells, was observed with the linked heterodimeric compounds. *In vitro* regeneration of active monomeric drugs was observed in a reducing environment with these dimeric prodrugs, with the superior leaving group promoting more facile release from the tether. These release trends were mirrored in the efficacy of the *in cyto* anti-HIV-1 activity of the Trojan horse heterodimers.

1. Introduction

HIV treatment has progressed substantially since the first documented case with combination antiretroviral therapies (cART) successfully reducing of plasma viral levels below the detectable limit.[1] Although cART has been a significant advancement in HIV treatment, HIV has not been eradicated due, in part, to viral reservoirs.[2-3] These viral reservoirs exist in a number of cellular and anatomical locations, including the central nervous system (CNS), macrophages and lymphocytes. Viral accumulation in the brain, for instance, has been proposed to mainly proceed through paracellular or transcellular diapedesis.[4] While HIV is able to enter the brain through these mechanisms, numerous cART treatments do not accumulate well in the brain due to the physiochemical properties of the drugs, the presence of tight junctions, and the high concentration of efflux transporters at the blood brain barrier (BBB).[5-7] One of the well studied efflux transporter, P-glycoprotein (P-gp), resides in the apical membrane of brain capillary endothelial cells where it is known to efflux many therapies.[8-9]

P-gp has many substrates, including various cART drugs targeting HIV-1 protease (PR), reverse transcriptase (RT), and integrase (IN). *In vitro* and *in vivo* experiments confirm that RT inhibitor drugs, such as abacavir, PR inhibitors, such as nelfinavir and darunavir, and IN inhibitor drugs, such as raltegravir, for instance, are P-gp substrates.[6,10-16] Notably, in P-gp null mice studies, abacavir and nelfinavir accumulated in the brain at increased levels as compared to wild-type mice (20-fold and 36-fold, respectively).[10,17] Further, chemical inhibition of P-gp efflux with a known inhibitor, LY-

335979, was shown to increase the brain accumulation of four different PR inhibitors (PI) *in-vitro* and *in-vivo*.[18] Such studies strongly support the hypothesis that P-gp efflux limits the accumulation of cART drugs in the brain, leaving viral replication unchecked.

An x-ray structure of P-gp has shown a large binding site region that can accommodate the binding of two cyclic peptides.[19-20] To block P-gp efflux, we wished to take advantage of this multiplicity of binding sites within the transmembrane domain of P-gp.[19-26] In this way we envisioned that taking two antiviral agents that are substrates of P-gp and combining them into the same molecule with a linker, would allow the heterodimeric compounds to occupy the multiple binding sites within P-gp, thereby turning 2 two substrates into one inhibitor. Dimerizing a P-gp substrate has been demonstrated to be an effective means to inhibit P-gp efflux in cells and *in situ* at the BBB.[27-36] Using this concept for antiviral substrates, reversibly linked homodimeric prodrugs of abacavir demonstrated potent P-gp inhibition with cellular anti-HIV-1 activity.[32] This proof of concept study paved the way for the current Trojan horse (TH) design (Figure 1), a reversible combination therapy in one molecule that also may act as a P-gp inhibitor to improve cell accumulation. Specifically, agents were designed as an cART prodrug containing the RT inhibitor (RTI) abacavir (Aba) and one of two PR inhibitors (PI), nelfinavir (NFV) or darunavir (DRV), linked via a disulfide-containing tether. Such compounds were designed to inhibit P-gp efflux and, in the reducing environment of an HIV infected cell, release two monomeric therapies within the cell. Herein, we discuss the successful synthesis and application of two cART heterodimers, Abacavir-S₂-Nelfinavir (Aba-S₂-NFV1) and Abacavir-S₂-Darunavir (Aba-S₂-DRV8), as P-

gp inhibitors and antiviral prodrugs, that highlight the importance of the chemical connectivity on their antiviral activity.
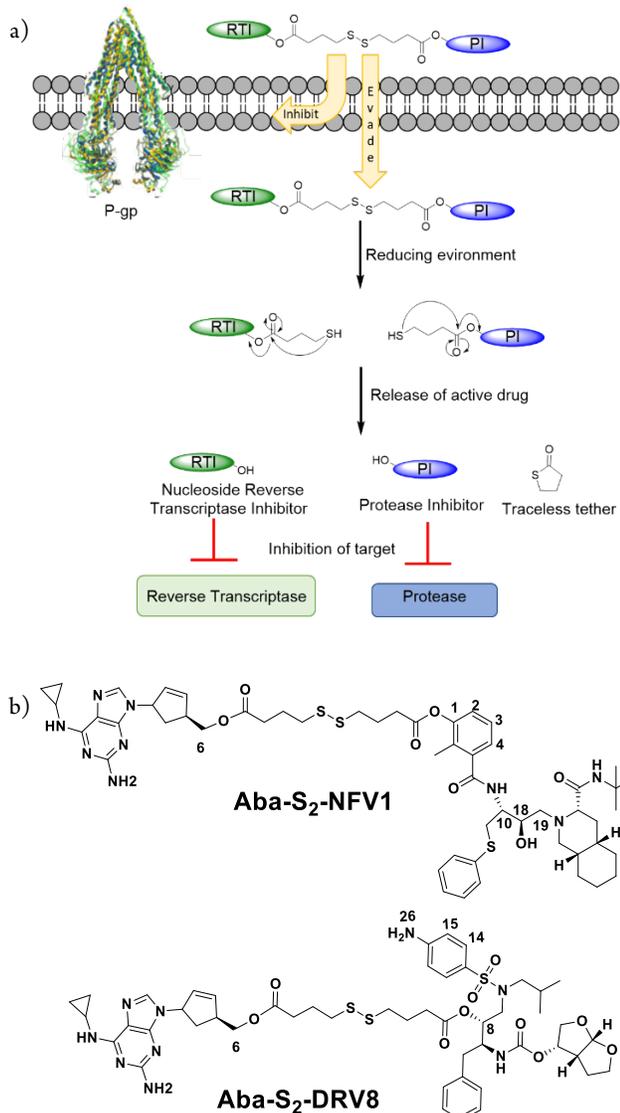
a)

b)

Figure 1. (a) Design of Trojan horse (TH) prodrugs containing a reverse transcriptase inhibitor (RTI), abacavir (Aba), a protease inhibitor (PI) (nelfinavir (NFV) or darunavir (DRV)) and a disulfide-containing tether. (b) Structures of Abacavir-S_2-Nelfinavir-1 (Aba-S_2-NFV1) and Abacavir-S_2-Darunavir-8 (Aba-S_2-DRV8).

2. Results and Discussion

2.1 Design. TH combination cART prodrugs were designed to provide two functions (1) inhibit P-gp efflux in brain endothelial cells and T-cells and (2) in the reducing environment of cells, release the monomeric therapies for interaction with target enzymes (Figure 1). This was accomplished by conjugating two classes of known FDA approved HIV-1 drugs, a RTI (Aba) and PIs (NFV and DRV) connected by ester linkages via a disulfide-containing tether. This tether contains a central disulfide moiety that is reduced in the reducing environment of the cell. The thiols that are generated can then rearrange to release the monomeric drugs of interest within the cell. Thus, the design creates TH heterodimers that may be useful tools in the treatment of cellular and anatomical reservoirs of HIV-1.
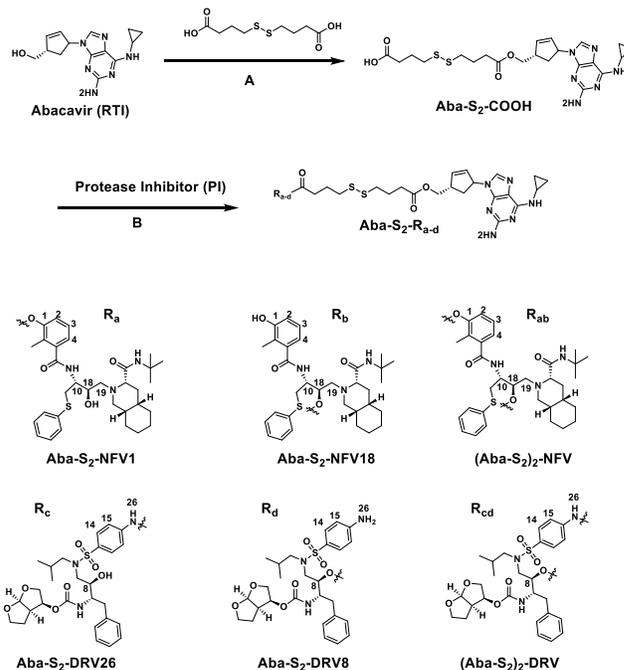
Scheme 1. Synthesis of Aba-S_2-NFV and Aba-S_2-DRV analogs A) PyBOP, DMAP, DIEA, DMF, RT 24 hr, 70% yield; B) EDC, DMAP, DIEA, CH$_2$Cl$_2$, 4 Å molecular sieves, 0 °C for 2 h, RT for 48 h; Aba-S_2-NFV1, 62% yield; Aba-S_2-NFV18, 3% yield; and (Aba-S_2)$_2$-NFV, 2% yield. Aba-S2-DRV8, 27% yield; (Aba-S_2)$_2$-DRV, 21% yield. Atom numbering used for NMR analysis of Aba-S_2-COOH, darunavir and nelfinavir derivatives.

2.2 Synthesis and characterization of TH dimers Aba-S_2-Nelf and Aba-S_2-Darun. The TH heterodimers were synthesized over two-steps. The presence of an alcohol functional group within Aba and NFV (C1 and C18) or DRV (C8) allowed us to introduce ester linkages to generate Aba-S_2-NFV and Aba-S_2-DRV analogs (Scheme 1).

In the first step of the synthesis of the heterodimers, Aba was treated with PyBOP-activated 4,4′-dithiodibutyric acid in the presence of DMAP and DIEA to produce Aba-S_2-COOH (Scheme 1) in 70% yield after purification by reverse phase HPLC (RP-HPLC). The selective acylation of the primary alcohol in Aba was established based on the resonances corresponding to the H-6 proton and the C-6 carbon of Aba-S_2-COOH, that were shifted downfield from the corresponding proton H-6 and carbon C-6 signals in Aba by 0.7 ppm (4.1 ppm from 3.4 ppm) and 2.7 ppm (66.9 ppm from 64.2 ppm), respectively (Figure S3-S6).

Acylation of NFV with Aba-S_2-COOH was accomplished using the PI and Aba-S_2-COOH in the presence of EDC/DMAP (Scheme 1). NFV has two possible sites of acylation –C1 (phenolic) and C18 (secondary hydroxyl) – that could potentially lead to 3 products: monoesters at C1 (Aba-S_2-NFV1) and C18 (Aba-S_2-NFV18), and a diester at both sites (Aba-S_2)$_2$-NFV (Scheme 1). Upon RP-HPLC separation, Aba-S_2-NFV1 was isolated in 62% yield with < 5% of the other possible ester derivatives obtained. The structure of Aba-S_2-NFV1 was elucidated by ^{1}H and ^{13}C NMR spectroscopy, with peak assignments confirmed using COSY, TOCSY, HMQC and HMBC NMR (Figure S7-S16). The acylation of the phenolic alcohol of NFV in Aba-S_2-NFV1 was confirmed by the observed deshielding of the protons H-2, H-3 and H-4, by 0.41 ppm, 0.22 ppm and 0.31 ppm,

respectively, as compared to the parent NFV (Figure S14). The formation of the phenyl ester was further confirmed by ^{13}C NMR, with shielding of the C-1 carbon signal by 6.4 ppm in Aba-S$_2$-NFV1 as compared to NFV (Figure S15),[37] and the deshielding of C-2, C-3 and C-4 by 8-13 ppm (Figure S15). Furthermore, ^{1}H and ^{13}C resonances in the vicinity of the secondary alcohol (H-10/C-10, H-18/C-18 and H-19/C-19) showed no significant change in the spectra of Aba-S$_2$-NFV1 as compared to NFV (Figure S16). These NMR data taken together confirm the structure of Aba-S$_2$-NFV1 as the phenyl ester derivative.

The acylation of DRV was accomplished as described above (Scheme 1). DRV, like NFV, has two possible conjugation locations, the secondary alcohol on C8 (Aba-S$_2$-DRV8) or the aniline N26, with the possible acylation at both sites ((Aba-S$_2$)$_2$-DRV). Upon RP-HPLC separation of the reaction mixture, Aba-S$_2$-DRV8 was obtained in 27% yield with the diacylated product ((Aba-S$_2$)$_2$-DRV) in 21% yield. The structure of Aba-S$_2$-DRV8 was also elucidated by ^{1}H and ^{13}C NMR spectroscopy using COSY, TOCSY and HMQC NMR (Figure S17-S24). The acylation of the secondary alcohol of darunavir in Aba-S$_2$-DRV8 was confirmed by the observed deshielding of the protons H-8 by 1.5 ppm, as compared to the parent darunavir (Figure S22). The formation of secondary ester was further confirmed by ^{13}C NMR with the deshielding of the C-8 signal by 2.3 ppm in Aba-S$_2$-DRV8 as compared to DRV (Figure S23). Furthermore, ^{1}H and ^{13}C NMR resonances in the vicinity of the aniline nitrogen (H-14/C-14 and H-15/C-15) showed no significant change in Aba-S$_2$-DRV8 as compared to DRV (Figure S24). These NMR data taken together confirmed that acylation proceeded on the secondary alcohol of darunavir. (Data for diacylated darunavir not shown). In all, this synthetic method allowed the preparation of two TH heterodimers, Aba-S$_2$-NFV1 and Aba-S$_2$-DRV8, for biological analysis.

2.3 Inhibition of P-gp efflux with Aba-S$_2$-NFV1 and Aba-S$_2$-DRV8.
One of the goals of the designed TH heterodimers is to inhibit P-gp-mediated efflux. A substrate accumulation assay was used to evaluate the potency of Aba-S$_2$-NFV1 and Aba-S$_2$-DRV8 as P-gp inhibitors using the P-gp substrates calcein-AM and NBD-Aba.[38-39] Two cell lines were used to monitor the accumulation of these fluorescent P-gp substrates: 12D7-MDR cells which are CD4+ T lymphocytes with overexpression of P-gp,[40] and hCMEC/D3 cells as an *in vitro* BBB model cell line.[41] hCMEC/D3 cells are an immortalized human brain capillary endothelial cell line that expresses endogenous levels of P-gp.[42-43] Inhibition of P-gp efflux was measured by monitoring the increase in cellular fluorescence with added heterodimer by flow cytometry. While the dimeric prodrugs have limited water solubility,

they were fully soluble in 1% DMSO up to 100 μM, and, therefore, the cell-based P-gp experiments used 1% DMSO with no observed cytotoxicity.

With the 12D7-MDR and hCMEC/D3 cell lines, Aba-S$_2$-NFV1 and Aba-S$_2$-DRV8 demonstrated dose-dependent, potent inhibition of P-gp efflux of calcein-AM and NBD-Aba with sub-micromolar IC$_{50}$ values (Table 1). Aba-S$_2$-DRV8 was the more potent of the two dimers with IC$_{50}$ values of 80-90 nM in hCMEC/D3 cells. Interestingly, the IC$_{50}$ values obtained with the hCMEC/D3 cells are lower than 12D7-MDR cells, especially with Aba-S$_2$-DRV8, likely due to the lower expression of P-gp in the brain capillary endothelial cells. Analogous experiments were performed with monomeric NFV and DRV using the fluorescent substrates. About a 3- to 12-fold increase in inhibition of P-gp was found with Aba-S$_2$-NFV1 as compared to NFV, and a striking 66- to 118-fold increase in inhibition of P-gp was found for Aba-S$_2$-DRV8 with respect to DRV alone (Table 1). Abacavir has been shown to minimally inhibit (<10%) P-gp in 12D7-MDR in cells up to 500 μM in these assays, whereas the known P-gp inhibitor verapamil had an IC$_{50}$ value of 1.2 ± 0.4 μM in 12D7-MDR cells with the calcein-AM substrate .[32] These data substantiate that the TH heterodimers are inhibitors of P-gp efflux in both T-cells and in a BBB cell model. Together, these IC$_{50}$ data confirm that the dimerization of two antivirals that are P-gp substrates – Aba and DRV/NFV – into one molecule successfully led to the generation of potent P-gp inhibitors.

An MTT assay was used to determine the cell toxicity of Aba-S$_2$-NFV1 and Aba-S$_2$-DRV8 in the 12D7-MDR cell lines after 24 hours.[44] In this assay, Aba-S$_2$-NFV1 demonstrated high cell viability (>95%) at the maximum concentration used (20 μM). Aba-S$_2$-DRV8, though slightly more cytotoxic than Aba-S$_2$-NFV1, still maintained 70% cell viability at 20 μM, which is 40 times its IC$_{50}$ for inhibition of P-gp. These data suggest that the TH heterodimers are minimally cytotoxic to 12D7-MDR cells at bioactive concentrations and can be used for further biological assays without detrimental effect on cell growth.

2.4 Probing the reversion of TH heterodimers into monomers in a reducing environment.
In a reducing environment the disulfide bonds within the TH heterodimers would yield 2 thiols (Figure 1a) that may rearrange to produce monomeric drugs (Aba, NFV and DRV). The breakdown of the TH heterodimers with DTT and glutathione (GSH), and the release of monomers was monitored using UPLC-MS at various timepoints. The reduction of the heterodimers to free thiols occurs rapidly, with full reduction observed within 1 hour. Upon appearance of free thiols, the subsequent rearrangement

Table 1. Inhibition of P-gp mediated efflux of calcein-AM and NBD-Aba in 12D7-MDR and hCMEC/D3 cells[a]

	IC$_{50}$ (μM)			
	12D7-MDR cells		hCMEC/D3 cells	
Compound	calcein-AM	NBD-Aba	calcein-AM	NBD-Aba
NFV	9.1 ± 3.0	5.8 ± 1.4	2.0 ± 0.2	1.7 ± 0.3
Aba-S$_2$-NFV1	0.77 ± 0.05	0.65 ± 0.09	0.59 ± 0.07	0.41 ± 0.06
DRV	33.2 ± 6.5	60 ± 9.4	6.6 ± 1.9	15.4 ± 3.2
Aba-S$_2$-DRV8	0.50 ± 0.04	0.51 ± 0.08	0.08 ± 0.02	0.09 ± 0.02

[a] Cells were treated with calcein-AM (0.25 μM) or NBD-Aba (5 μM) with different concentrations of compound. The accumulated fluorescence was analyzed using flow cytometery.

led to the generation of the component monomeric drugs. Aba regeneration from each TH heterodimer (Aba-S$_2$-NFV1 and Aba-S$_2$-DRV8) was consistent between heterodimers with a half-life (t$_{1/2}$) of 31.8 ± 6.8 and 34.5 ± 1.5 hours, respectively with DTT, and 29.4 ± 3 and 21.6 ± 2 hours, respectively with with GSH. DRV and NFV were regenerated with a t$_{1/2}$ of 21.3 ± 0.8 and 1.2 ± 0.2 hours with DTT, respectively, and 36.3 ± 4 and 10.3 ± 1 hours with GSH. Interestingly, NFV was released significantly faster than the release of DRV and Aba. This significant difference in monomer release is likely due to the differences in the chemical connectivity of the monomers. NFV, as described above, is connected to the tether via a phenolic moiety, whereas DRV is linked by a secondary alcohol. The better leaving group ability of the phenol versus the secondary alcohol likely leads to the observed difference in monomer regeneration.

2.5 The anti-HIV-1 potency of each TH heterodimer as compared to their monomers, alone and combined. To investigate if Aba-S$_2$-NFV1 and Aba-S$_2$-DRV8 are effective against HIV-1 in cells, an *in vitro* HIV-1 titer assay was performed using the 12D7 cell line. 12D7 cells were infected with HIV-1$_{LAI}$ and anti-HIV-1 activity was measured by monitoring p24 protein levels as previously described.[45-46] First the stability of the prodrugs was monitored in PBS and cell culture media using UPLC-MS. Aba-S$_2$-NFV1 was greater than 95% intact after 1 week under both condition, whereas Aba-S$_2$-DRV8 was also greater than 95% intact after 3 days under both conditions, but with decomposition observed after day 4. Therefore, for the cell-based anti-HIV-1 experiments, the media, with drugs, was changed every 3 days. The anti-HIV-1 activity of different concentrations of monomeric drugs alone (Aba, NFV or DRV), 1:1 combinations of an RTI with a PI (Aba and NFV or Aba and DRV) or the TH heterodimer was determined after 6 days. All drugs and drug combinations demonstrated a decrease in p24 levels as compared to the control, which corresponds to an increase in anti-HIV-1 activity. The PIs used are known to be superior antivirals as compared to the RTI Aba,[47] and this was also observed (Figure 2). Therefore, the antiretroviral activity of the 1:1 mix of Aba with NFV or DRV was dominated by the PI potency. For the TH heterodimers, the anti-HIV-1 activity of Aba-S$_2$-NFV was similar to the 1:1 mixture of Aba and NFV, whereas Aba-S$_2$-DRV was less potent than the 1:1 mixture of Aba and DRV. DRV alone is a highly potent antiviral and is more potent than NFV alone[48] (Figure 2). Therefore, one might expect that Aba-S$_2$-DRV8 would have superior anti-HIV-1activity as compared to Aba-S$_2$-NFV1. However, the release of NFV from Aba-S$_2$-NFV1 is 18-fold faster than DRV release from Aba-S$_2$-DRV8 due to the better phenolic leaving group. Thus, this difference in chemical connectivity leads to a difference in monomer release, that may be responsible for the differences in anti-HIV-1 potency.

3. Conclusion

Herein, the successful synthesis and application of two TH heterodimers, Aba-S$_2$-NFV1 and Aba-S$_2$-DRV8, as P-gp inhibitors and antiviral prodrugs is discussed. Each heterodimer was synthesized and the connectivity points within the monomers was fully characterized by NMR. Both TH heterodimers are potent P-gp inhibitors with activity in T-cells and endothelial cells from the BBB. These dimers were found to revert to their component monomers (Aba, NFV and DRV) in a reducing environment, with NFV releasing significantly faster than DRV. Both TH heterodimers displayed anti-HIV-1 activity in T cells, with Aba-S$_2$-NFV1 displaying superior potency as compared to Aba-S$_2$-DRV8. The quicker regeneration of monomeric
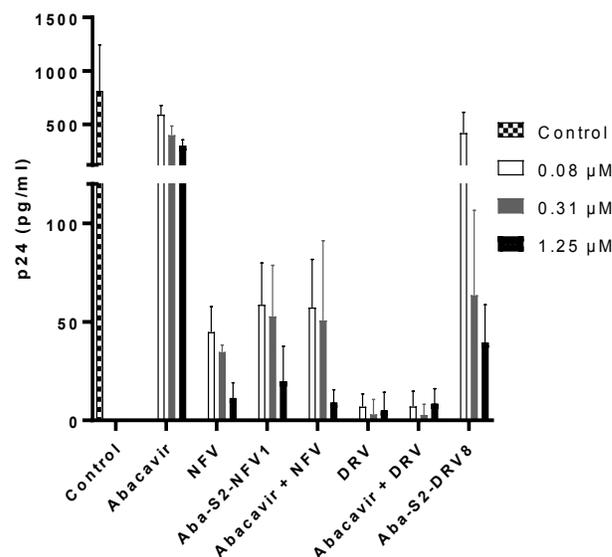

Figure 2. Anti-HIV-1 activity of individual RTI or PI antivirals, a 1:1 mixture of RTI and PI, and the TH heterodimers in HIV-1$_{LAI}$ infected 12D7 cells. The plotted data is the average of HIV-1 p24 with the standard deviation derived from two independent experiments.

NFV in the reducing environment and, in turn, the superior anti-HIV potency of Aba-S$_2$-NFV1 as compared to Aba-S$_2$-DRV8, is likely due to the better phenolic leaving group in Aba-S$_2$-NFV. Thus, chemical connectivity to the tether within these TH heterodimers has a notable effect on the observed anti-HIV-1 activity. Future studies may probe alternate linking chemistry to promote more facile release of the combination therapies from the TH prodrugs.

4. Experimental

4.1 Materials. Abacavir, darunavir and nelfinavir were provided by the NIH AIDS Reagent Program (Germantown, MD). ((1H-benzo[d][1,2,3]triazol-1-yl)oxy)tri(pyrrolidin-1-yl)phosphonium hexafluorophosphate (PyBOP) was bought from GenScript Corporation (Piscataway, NJ). DTT was purchased from Roche (Indianapolis, IN). 1-(3-Dimethylaminoproyl)-3-ethylcarbodiimide hydrochloride (EDC) was purchased fom AK Scientific (Union City, CA). 4,4′-Dithiodibutyric acid,N,N-dimethylpyridin-4-amine (DMAP) and N-ethyl-N-isopropylpropan-2-amine (DIEA) were purchased from Sigma-Aldrich (St. Louis, MO). hCMEC/D3 cells were donated from Institut National de la Sante et de la Recherche Medicale (INSERM, Paris, France). Rat tail collagen I was purchased from BD Biosciences (San Jose, CA). EBM-2 growth medium was purchased from Lonza (Basel, Switzerland). Calcein-AM was bought from Invitrogen (Carlsbad, CA), All other reagents were either purchased from Sigma Aldrich (St. Louis, MO). or Invitrogen (Carlsbad, CA) and used without further purification. ^{1}H, ^{13}C, and 2D NMR spectra were recorded with a Bruker AC 800 and Bruker AC 500 MHz. DMSO-*d6* was used to prepare NMR samples.

4.2 Methods

Synthesis of Aba-S$_2$-COOH

To a solution of 4,4′-dithiodibutyric acid (400 mg, 1.7 mmol) was added PyBOP (114 mg, 0.22 mmol), DIEA (0.20 ml, 0.75 mmol) and DMAP (2.6 mg, 0.022 mmol) under nitrogen atmosphere at room temperature in dry DMF (2 ml). After 20 min, abacavir sulfate

(50 mg, 0.15 mmol) was added. The mixture was left to stir at room temperature for 24 hours. The resulting reaction mixture was dissolved in DMSO and purified using RP-HPLC. The RP-HPLC solvent consisted of acetonitrile with 0.1 % TFA (solvent A) and water with 0.1 % TFA (solvent B). A gradient of 20–70% of solvent A with the flow rate of 12.0 mL/min and UV detection at 214 nm and 280 nm with a C8 column (Phenomenex, USA) was used for purification. Purity of the product (~99%) was estimated by C8 analytical RP-HPLC using a flow rate of 1.2 mL/min and UV detection at 214 and 280 nm and a gradient from 20-70% (solvent A) over 30 mins. The retention time for Aba-S$_2$-COOH was found to be 16.2 mins. The yield for this reaction was calculated to be 70%. Calculated mass for Aba-S$_2$-COOH 506.18, observed mass by ESI-MS 507.2 [M+H]$^+$.

Aba-S$_2$-COOH: ^{1}H NMR (500 MHz, DMSO-*d6*) δ 12.18 (s, 2H), 9.77 (s, 1H), 7.93 (s, 1H), 7.45 (s, 2H), 6.13 (dd, J = 5.3, 2.5 Hz, 1H), 5.98 (dt, J = 5.1, 2.2 Hz, 1H), 5.43 (ddd, J = 8.6, 6.1, 2.4 Hz, 1H), 4.09 (d, J = 6.1 Hz, 2H), 3.11 (ddt, J = 12.0, 8.5, 4.1 Hz, 1H), 2.85 (s, 1H), 2.68 (qd, J = 8.1, 7.2, 4.4 Hz, 5H), 2.38 (td, J = 7.3, 4.4 Hz, 2H), 2.29 (t, J = 7.2 Hz, 2H), 1.82 (dp, J = 11.4, 7.2 Hz, 4H), 1.62 (dt, J = 13.8, 5.9 Hz, 1H), 0.88 (s, 2H), 0.74 (s, 2H); ^{13}C NMR (126 MHz, DMSO-*d6*) δ 174.34, 172.85, 159.09, 158.84, 158.59, 137.79, 130.49, 118.60, 116.23, 66.72, 59.61, 45.70, 44.48, 40.48, 40.32, 40.15, 39.98, 39.82, 39.65, 39.48, 37.28, 37.10, 34.71, 32.54, 32.34, 26.07, 24.43, 24.40, 7.39.

Synthesis of Aba-S$_2$-NFV1

To a flame dried round bottom flask under nitrogen, was added NFV (20 mg, 34.8 µmol), Aba-S$_2$-COOH (21.5 mg, 34.8 µmol), EDC (10 mg, 52.2 µmol), DMAP (8.5 mg, 69.7 µmol), DIEA (60µl, 348 µmol) and 4 Å powdered molecular sieves followed by dry DCM (1 ml) at 0 °C. The reaction mixture was stirred at room temperature for 24 hours, and the progress of the reaction was monitored by RP-HPLC. An additional aliquot of EDC (10 mg, 52.2 µmol) was added after 24 hours and the reaction mixture was stirred for an additional 2 days. The mixture was diluted with DMSO and components separated by RP-HPLC on a C18 column (Phenomenex, USA) with a flow rate of 12 ml/min, a gradient of 20–60% solvent A over 60 min and UV detection at 214 nm and 254 nm. Aba-S$_2$-NFV1 was obtained (62% yield, major product) with Aba-S$_2$-NFV18 and (Aba-S$_2$)$_2$-NFV (5% yield, minor products). Aba-S$_2$-NFV1 (major product) had a purity of 99% by RP-HPLC (Figure S2), and the compound was fully characterized by NMR (see below and Figures S7-16). ESI-MS: calculated mass: 1056.5, observed mass: 1057.0; high resolution MS: calculated mass: 1056.4868, observed mass: 1056.4890.

Aba-S$_2$-NFV1: ^{1}H NMR (800 MHz, DMSO-*d6*) δ 9.85 (s, 1H), 9.20 (s, 1H), 8.37 (d, J = 8.9 Hz, 1H), 8.21 (s, 1H), 7.97 (s, 1H), 7.63 (s, 2H), 7.38 – 7.29 (m, 5H), 7.28 (t, J = 7.8 Hz, 1H), 7.23 – 7.19 (m, 1H), 7.16 (dt, J = 8.0, 1.9 Hz, 1H), 6.14 (dt, J = 5.7, 2.1 Hz, 1H), 5.98 (dt, J = 5.7, 2.2 Hz, 1H), 5.43 (ddd, J = 10.7, 4.8, 2.0 Hz, 1H), 4.14 – 4.05 (m, 3H), 3.94 (q, J = 10.5 Hz, 1H), 3.87 (s, 1H), 3.56 (d, J = 12.9 Hz, 1H), 3.41 (dd, J = 13.7, 2.9 Hz, 1H), 3.28 (s, 1H), 3.23 (d, J = 13.4 Hz, 1H), 3.10 (ddq, J = 8.3, 6.3, 2.1 Hz, 1H), 3.03 – 2.98 (m, 2H), 2.84 – 2.67 (m, 8H), 2.45 – 2.34 (m, 2H), 2.16 (d, J = 3.8 Hz, 3H), 2.08 – 1.98 (m, 2H), 1.96 – 1.90 (m, 3H), 1.86 (dp, J = 21.4, 7.2 Hz, 2H), 1.76 (m, 1H), 1.71 (d, J = 12.7 Hz, 2H), 1.63 (dt, J = 13.9, 5.9 Hz, 1H), 1.54 (t, J = 6.3 Hz, 2H), 1.40 (d, J = 12.4 Hz, 1H), 1.36 – 1.32 (m, 1H), 1.29– 1.15 (m, 11H), 0.92 – 0.88 (m, 2H), 0.78 (s, 2H). ^{13}C NMR (126 MHz, DMSO-d6) δ 172.85, 171.51, 169.09, 167.53, 158.91, 158.63, 152.99, 149.67, 139.23, 137.89, 136.34, 130.38, 129.55, 128.93, 128.21, 126.71, 126.44, 125.41, 123.90,

112.11, 68.91, 67.15, 66.72, 59.74, 58.96, 57.91, 52.60, 51.43, 44.48, 36.99, 34.68, 34.13, 33.99, 32.33, 32.25, 31.72, 30.21, 29.48, 28.84, 28.62, 25.99, 25.04, 24.37, 24.31, 23.61, 20.40, 13.32, 7.41.

Synthesis of Aba-S$_2$-DRV8

To a flame dried round bottom flask under nitrogen, was added DRV (20 mg, 36µmol), Aba-S$_2$-COOH (21.5 mg, 34.8 µmol), EDC (10 mg, 52.2 µmol), DMAP (8.5 mg, 69.7 µmol), DIEA (60µl, 348 µmol) and 4 Å powdered molecular sieves followed by dry DCM (1 ml) at 0 °C. The reaction mixture was stirred at room temperature for 72 hours, and the progress of the reaction was monitored by RP-HPLC. The reaction mixture was diluted with DMSO and components separated by RP-HPLC on a C18 column (Phenomenex, USA) with a flow rate of 12 ml/min, a gradient of 20–95% solvent A over 60 min and UV detection at 214 nm and 254 nm. Aba-S$_2$-DRV was obtained (27% yield, major product) with (Aba-S$_2$)$_2$-DRV (21% yield, minor product). The retention time of Aba-S$_2$-DRV8 (major product) had a purity of 99% (Figure S1), and the compound was fully characterized by NMR (see below and Figures S17-S24). ESI-MS: calculated mass: 1036.4, observed mass: 1036.8; high resolution MS: calculated mass: 1036.4089, observed mass: 1036.4106.

Aba-S$_2$-DRV8: ^{1}H NMR (800 MHz, DMSO-*d6*) δ 7.48 (d, J = 9.4 Hz, 1H), 7.39 (d, J = 8.7 Hz, 1H), 7.21 (dt, J = 15.3, 7.1 Hz, 3H), 7.16 – 7.13 (m, 1H), 6.61 (d, J = 8.7 Hz, 1H), 6.12 (dt, J = 5.6, 2.1 Hz, 1H), 5.96 (dt, J = 5.6, 2.2 Hz, 1H), 5.48 (d, J = 5.2 Hz, 1H), 5.41 (ddq, J = 8.2, 6.2, 2.1 Hz, 1H), 5.06 (ddd, J = 9.0, 4.5, 2.8 Hz, 1H), 4.84 (dt, J = 8.0, 5.8 Hz, 1H), 4.07 (dd, J = 6.2, 2.1 Hz, 2H), 3.95 (ddd, J = 14.9, 9.1, 4.1 Hz, 1H), 3.85 (dd, J = 9.6, 6.0 Hz, 1H), 3.69 (td, J = 8.2, 1.9 Hz, 1H), 3.56 (ddt, J = 16.4, 8.3, 5.6 Hz, 2H), 3.29 (dd, J = 15.4, 2.9 Hz, 1H), 3.08 (ddp, J = 8.3, 6.2, 2.0 Hz, 1H), 3.04 (dd, J = 15.3, 9.0 Hz, 1H), 2.81 (dt, J = 13.4, 3.8 Hz, 2H), 2.78 – 2.72 (m, 1H), 2.69 (dt, J = 18.8, 7.1 Hz, 4H), 2.60 – 2.51 (m, 1H), 2.50 – 2.47 (m, 3H), 2.42 – 2.38 (m, 1H), 2.38 – 2.30 (m, 3H), 2.06 (s, 0H), 1.91 – 1.85 (m, 2H), 1.83 (q, J = 7.3 Hz, 2H), 1.78 (ddt, J = 13.1, 9.0, 6.5 Hz, 1H), 1.61 (dt, J = 13.8, 5.9 Hz, 1H), 1.39 – 1.30 (m, 1H), 1.17 – 1.11 (m, 1H), 0.77 (dd, J = 6.6, 4.5 Hz, 5H). ^{13}C NMR (800 MHz, DMSO-*d6*) δ 172.82, 172.35, 155.81, 153.44, 138.77, 137.77, 130.46, 129.56, 129.52, 128.48, 126.54, 123.29, 113.18, 109.22, 109.20, 75.08, 73.07, 70.65, 69.25, 66.72, 59.60, 57.73, 53.72, 49.50, 45.47, 44.45, 40.29, 40.18, 40.08, 39.97, 39.87, 39.77, 39.66, 37.08, 37.05, 35.56, 34.68, 32.51, 32.30, 26.82, 25.89, 24.34, 24.07, 23.56, 20.37, 20.21.

Cell Culture

12D7-MDR cells were grown in complete RPMI 1640 media with vincristine (0.5 ng/mL), 50 units/mL of penicillin and 50µg/mL streptomycin, 5 mM of L-glutamine and 10 % FBS. The growth of cells was maintained at 37 ° C in 5% CO$_2$. hCMEC/D3 cells were cultured according to literature protocols with minor modifications.[41] The media used for growth consisted of endothelial growth medium-2 (EGM-2) supplemented with 5% fetal bovine serum, 1 % penicillin-streptomycin, 0.5% human basic fibroblast growth factor (hbFGF), 1.4 µM hydrocortisone, 5 µg/mL ascorbic acid, 1% (10 mM) HEPES and 1% lipid concentrate.

Flow Cytometry Assay

Flow cytometry was used to estimate P-gp inhibition using a substrate accumulation assay as described previously with some minor changes.[38] BME media (with fluorescent P-gp substrate) along with the compound of interest in DMSO (1%) was added to 125,000 cells in suspension and stored in a CO$_2$ incubator at 37 °C for 30 mins. The cells were harvested by centrifugation at 300 x g at 4 °C for 7

mins. The supernatant was carefully removed, and 400 µl of cold, sterile PBS was added to the cell pellet. The accumulation of calcein-AM or NBD-Aba was measured using a FACSCalibur flow cytometer (BD Biosciences) with an excitation wavelength of 488 nm argon laser and an emission 530 nm bandpass filter (FL1). The mean fluorescence value for each concentration corresponded to 10,000 cells. Each sample was run in duplicate and all the experiments were run in duplicates on two different days. The average fluorescence accumulated in the cells for samples was used to plot the mean fluorescence vs. concentration, and the IC_{50} values were estimated using the Graph Pad Prism.

Cell Viability Assay

The viability of 12D7-MDR cells in the presence of a TH heterodimer (Aba-S_2-NFV1 or Aba-S_2-DRV8) was measured using the standard MTT assay.[44] 20,000 12D7-MDR cells were plated in 96-well plate in 100 µL of cell media. After 12 hours, TH heterodimer in media was added to each well to give a final concentration of 5, 10 and 20 µM (1% DMSO). After 24 hours 20 µl of MTT in PBS (5 mg/mL) was added to all the wells and incubated for 2.5 hours. The 96 well plates were centrifuged at 300 x g for 7 mins, followed by careful removal of supernatant. 100 µl of DMSO was added to dissolve the formazan. The absorbance of the DMSO solution was read using plate reader at 590 nm. Cell viability was reported as the ratio of absorbance of cells treated with TH heterodimer relative to cells treated with DMSO.

Stability of TH heterodimers with DTT

Stability studies with DTT and GSH were adapted from a previously published protocol with some changes.[32] Aba-S_2-NFV1 and Aba-S_2-DRV8 (4 µM) were incubated at 37 °C with 250 mM DTT or 10 mM GSH in degassed 30% methanol/ PBS (pH ~7.4) containing 5 µM quinine as the internal standard. When monitoring NFV and DRV release, an aliquot of the reaction mixture was taken at different time points and directly analyzed by UPLC-MS. For analysis of Aba release, an aliquot of reaction mixture was taken and stored at -80 °C before analysis. The time points were analyzed using RP-UPLC with a C18 column consisting of solvent A (water and 0.1% formic acid) and solvent B (acetonitrile and 0.1% formic acid), a gradient of 5-95% of solvent B over 10 mins and a flow rate of 0.5 ml/min. The peaks corresponding to m/z for quinine (325.4), Aba-S_2-NFV1 (1056.4), Aba-S_2-DRV8 (1036.5), Aba-SH (389.4), Aba (287.4), NFV (568.6) and DRV (548.4) were detected and extracted using MassLynx software. The experiments were run in duplicate, and the average percentage of release vs time was fitted using Graph Pad Prism 7 to generate $t_{1/2}$'s.

Stability of Aba-S_2-NFV1 and Aba-S_2-DRV8 in cell culture media

The cell media stability studies for the TH heterodimers (Aba-S_2-NFV1 or Aba-S_2-DRV8) was carried out following a previously published protocol with some modifications.[32] Heterodimers (100 µM) were incubated at 37 °C in the cell media used for 12D7 cells (complete RPMI 1640 media with 50 units/mL of penicillin and 50µg/mL streptomycin, 5 mM of L-glutamine and 10 % FBS) with 1% DMSO. Every 24 hours ice-cold acetonitrile with 4-methoxybenzyl alcohol (1.0 mM) was added to an aliquot of the reaction mixture (1:1). The resultant solution was vortexed for 1 min, sonicated for 10 mins and centrifuged twice at 10000 x g for 10 mins each. The supernatant was stored at -80 °C. All samples were analyzed using a C8 analytical column (Phenomenex, USA) on RP-HPLC with eluent consisting of solvent A (water and 0.05% TFA) and solvent B (acetonitrile and 0.05% TFA). A gradient of 15-75% solvent B over

30 min with a flow rate of 1.2 ml/min and UV detection at 254 nm was used. The assays were performed in duplicate.

HIV-1 cell inhibition assay

12D7 cells were grown in the identical media for the cell culture media stability studies. The cells in log-phase were pelleted and resuspended at 1 million cells per ml. 500 $TCID_{50}$ HIV-1_{LAI} was used to infect cells for 4 hours using a known procedure.[45] These infected cells were plated at a density of 75,000 cells per ml in 48-well plates after three washes with the media. Different concentrations of the compound of interest were added keeping the DMSO concentration at 0.05%. After three days, the media was replaced with fresh media containing the same concentration of the compound of interest. On the 6th day, the supernatant was analyzed using ELISA to quantify the amount of HIV-1 p24 (gag) protein generated in each sample.[46] All assays were run in duplicate.

ASSOCIATED CONTENT

AUTHOR INFORMATION

Corresponding Author

*J. Chmielewski, chml@purdue.edu

ABBREVIATIONS

HIV, human immunodeficiency virus; cART, combination antiretroviral therapy; CNS, central nervous system; BBB, blood brain barrier; P-gp, P-glycoprotein; PR, HIV protease; RT, HIV reverse transcriptase; IN, HIV integrase inhibitor; TH, Trojan horse; RTI, reverse transcriptase inhibitor; PI, protease inhibitor; Aba, abacavir; DRV, darunavir; NFV, nelfinavir; Aba-S_2-NFV1, Abacavir-S_2-Nelfinavir1; Aba-S_2-DRV8, Abacavir-S_2-Darunavir8; PyBOP, benzotriazole-1-yl-oxytripyrrolidino-phosphonium hexafluorophosphate; DMAP, 4-dimethylaminopyridine; DIEA, N,N-diisopropylethylamine; DMF, N,N-dimethylformamide; DCM, dichloromethane; RP-HPLC, reverse phase-high performance liquid chromatography; ESI-MS, electrospray ionization-mass spectrometry; NMR, nuclear magnetic resonance; DEPT, distortionless enhancement by polarization transfer; COSY, correlated spectroscopy;

HMQC, heteronuclear multiple-quantum correlation; HMBC, heteronuclear multiple bond correlation; TOCSY, total correlated spectroscopy; MTT, 1-(4,5-dimethylthiazol-2-yl)-3,5-diphenylformazan; DTT, dithiothreitol; GSH, glutathione; UPLC-MS, ultra performance liquid chromatography-mass spectrometry; MALDI-TOF, matrix assisted laser desorption/ionization-time of flight

REFERENCES

1. Autran, B.; Carcelain, G.; Li, T. S.; Blanc, C.; Mathez, D.; Tubiana, R.; Katlama, C.; Debré, P.; Leibowitch, J. Positive Effects of Combined Antiretroviral Therapy on CD4+ T Cell Homeostasis and Function in Advanced HIV Disease. *Science* **1997**, *277* (5322), 112–116.

2. Lambotte, O.; Deiva, K.; Tardieu, M. HIV-1 Persistence, Viral Reservoir, and the Central Nervous System in the HAART Era. *Brain Pathol. Zurich Switz.* **2003**, *13* (1), 95–103.

3. Pierson, T.; McArthur, J.; Siliciano, R. F. Reservoirs for HIV-1: Mechanisms for Viral Persistence in the Presence of Antiviral Immune Responses and Antiretroviral Therapy. *Annu. Rev. Immunol.* **2000**, *18*, 665–708.

4. Ivey, N. S.; MacLean, A. G.; Lackner, A. A. Acquired Immunodeficiency Syndrome and the Blood-Brain Barrier. *J. Neurovirol.* **2009**, *15* (2), 111–122.

5. Thomas, S. A. Anti-HIV Drug Distribution to the Central Nervous System. *Curr. Pharm. Des.* **2004**, *10* (12), 1313–1324.

6. Varatharajan, L.; Thomas, S. A. The Transport of Anti-HIV Drugs across Blood-CNS Interfaces: Summary of Current Knowledge and Recommendations for Further Research. *Antiviral Res.* **2009**, *82* (2), A99-109.

7. Kandanearatchi, A.; Williams, B.; Everall, I. P. Assessing the Efficacy of Highly Active Antiretroviral Therapy in the Brain. *Brain Pathol.* **2003**, *13* (1), 104–110.

8. Schinkel, A. H. P-Glycoprotein, a Gatekeeper in the Blood-Brain Barrier. *Adv. Drug Deliv. Rev.* **1999**, *36* (2–3), 179–194.

9. Saidijam, M.; Karimi Dermani, F.; Sohrabi, S.; Patching, S. G. Efflux Proteins at the Blood-Brain Barrier: Review and Bioinformatics Analysis. *Xenobiotica.* **2018**, *48* (5), 506–532.

10. Shaik, N.; Giri, N.; Pan, G.; Elmquist, W. F. P-Glycoprotein-Mediated Active Efflux of the Anti-HIV1 Nucleoside Abacavir Limits Cellular Accumulation and Brain Distribution. *Drug Metab. Dispos.* **2007**, *35* (11), 2076–2085.

11. de Souza, J.; Benet, L. Z.; Huang, Y.; Storpirtis, S. Comparison of Bidirectional Lamivudine and Zidovudine Transport Using MDCK, MDCK-MDR1, and Caco-2 Cell Monolayers. *J. Pharm. Sci.* **2009**, *98* (11), 4413–4419.

12. Lee, C. G.; Gottesman, M. M.; Cardarelli, C. O.; Ramachandra, M.; Jeang, K. T.; Ambudkar, S. V.; Pastan, I.; Dey, S. HIV-1 Protease Inhibitors Are Substrates for the MDR1 Multidrug Transporter. *Biochemistry* **1998**, *37* (11), 3594–3601.

13. Bousquet, L.; Roucairol, C.; Hembury, A.; Nevers, M.-C.; Creminon, C.; Farinotti, R.; Mabondzo, A. Comparison of ABC Transporter Modulation by Atazanavir in Lymphocytes and Human Brain Endothelial Cells: ABC Transporters Are Involved in the Atazanavir-Limited Passage across an in Vitro Human Model of the Blood-Brain Barrier. *AIDS Res. Hum. Retroviruses* **2008**, *24* (9), 1147–1154.

14. Fujimoto, H.; Higuchi, M.; Watanabe, H.; Koh, Y.; Ghosh, A. K.; Mitsuya, H.; Tanoue, N.; Hamada, A.; Saito, H. P-Glycoprotein Mediates Efflux Transport of Darunavir in Human Intestinal Caco-2 and ABCB1 Gene-Transfected Renal LLC-PK1 Cell Lines. *Biol. Pharm. Bull.* **2009**, *32* (9), 1588–1593.

15. Gimenez, F.; Fernandez, C.; Mabondzo, A. Transport of HIV Protease Inhibitors through the Blood-Brain Barrier and Interactions with the Efflux Proteins, P-Glycoprotein and Multidrug Resistance Proteins. *J. Acquir. Immune Defic. Syndr.* **2004**, *36* (2), 649–658.

16. Hashiguchi, Y.; Hamada, A.; Shinohara, T.; Tsuchiya, K.; Jono, H.; Saito, H. Role of P-Glycoprotein in the Efflux of Raltegravir from Human Intestinal Cells and CD4+ T-Cells as an Interaction Target for Anti-HIV Agents. *Biochem. Biophys. Res. Commun.* **2013**, *439* (2), 221–227.

17. Kim, R. B.; Fromm, M. F.; Wandel, C.; Leake, B.; Wood, A. J.; Roden, D. M.; Wilkinson, G. R. The Drug Transporter P-Glycoprotein Limits Oral Absorption and Brain Entry of HIV-1 Protease Inhibitors. *J. Clin. Invest.* **1998**, *101* (2), 289–294.

18. Choo, E. F.; Leake, B.; Wandel, C.; Imamura, H.; Wood, A. J.; Wilkinson, G. R.; Kim, R. B. Pharmacological Inhibition of P-Glycoprotein Transport Enhances the Distribution of HIV-1 Protease Inhibitors into Brain and Testes. *Drug Metab. Dispos. Biol.* **2000**, *28* (6), 655–660.

19. Aller, S. G.; Yu, J.; Ward, A.; Weng, Y.; Chittaboina, S.; Zhuo, R.; Harrell, P. M.; Trinh, Y. T.; Zhang, Q.; Urbatsch, I. L.; Chang, G. Structure of P-Glycoprotein Reveals a Molecular Basis for Poly-Specific Drug Binding. *Science* **2009**, *323* (5922), 1718–1722.

20. Jin, M. S.; Oldham, M. L.; Zhang, Q.; Chen, J. Crystal Structure of the Multidrug Transporter P-Glycoprotein from Caenorhabditis Elegans. *Nature* **2012**, *490* (7421), 566–569.

21. Kim, Y.; Chen, J. Molecular Structure of Human P-Glycoprotein in the ATP-Bound, Outward-Facing Conformation. *Science* **2018**, *359* (6378), 915–919.

22. Bruggemann, E. P.; Currier, S. J.; Gottesman, M. M.; Pastan, I. Characterization of the Azidopine and Vinblastine Binding Site of P-Glycoprotein. *J. Biol. Chem.* **1992**, *267* (29), 21020–21026.

23. Shapiro, A. B.; Ling, V. Positively Cooperative Sites for Drug Transport by P-Glycoprotein with Distinct Drug Specificities. *Eur. J. Biochem.* **1997**, *250* (1), 130–137.

24. Dey, S.; Ramachandra, M.; Pastan, I.; Gottesman, M. M.; Ambudkar, S. V. Evidence for Two Nonidentical Drug-Interaction Sites in the Human P-Glycoprotein. *Proc. Natl. Acad. Sci.* **1997**, *94* (20), 10594–10599.

25. Loo, T. W.; Bartlett, M. C.; Clarke, D. M. Methanethiosulfonate Derivatives of Rhodamine and Verapamil Activate Human P-Glycoprotein at Different Sites. *J. Biol. Chem.* **2003**, *278* (50), 50136–50141.

26. Chufan, E. E.; Sim, H. M.; Ambudkar, S. V. Molecular Basis of the Polyspecificity of P-Glycoprotein (ABCB1): Recent Biochemical and Structural Studies. *Adv. Cancer Res.* **2015**, *125*, 71–96.

27. Sauna, Z. E.; Andrus, M. B.; Turner, T. M.; Ambudkar, S. V. Biochemical Basis of Polyvalency as a Strategy for Enhancing the Efficacy of P-Glycoprotein (ABCB1) Modulators: Stipiamide Homodimers Separated with Defined-Length Spacers Reverse Drug Efflux with Greater Efficacy. *Biochemistry* **2004**, *43* (8), 2262–2271.

28. Pires, M. M.; Hrycyna, C. A.; Chmielewski, J. Bivalent Probes of the Human Multidrug Transporter P-Glycoprotein. *Biochemistry* **2006**, *45* (38), 11695–11702.

29. Chan, K. F.; Zhao, Y.; Burkett, B. A.; Wong, I. L.; Chow, L. M.; Chan, T. H. Flavonoid Dimers as Bivalent Modulators for P-Glycoprotein-Based Multidrug Resistance: Synthetic Apigenin Homodimers Linked with Defined-Length Poly(Ethylene Glycol) Spacers Increase Drug Retention and Enhance Chemosensitivity in Resistant Cancer Cells. *Med. Chem.* **2006**, *49* (23), 6742–6759.

30. Pires, M. M.; Emmert, D.; Hrycyna, C. A.; Chmielewski, J. Inhibition of P-Glycoprotein-Mediated Paclitaxel Resistance by Reversibly Linked Quinine Homodimers. *Mol. Pharmacol.* **2009**, *75* (1), 92–100.

31. Kuriakose, J.; Hrycyna, C. A.; Chmielewski, J. Click Chemistry-Derived Bivalent Quinine Inhibitors of P-Glycoprotein-Mediated Cellular Efflux. *Bioorg. Med. Chem. Lett.* **2012**, *22* (13), 4410–4412.

32. Namanja, H. A.; Emmert, D.; Davis, D. A.; Campos, C.; Miller, D. S.; Hrycyna, C. A.; Chmielewski, J. Toward Eradicating HIV Reservoirs in the Brain: Inhibiting P-Glycoprotein at the Blood–Brain Barrier with Prodrug Abacavir Dimers. *J. Am. Chem. Soc.* **2012**, *134* (6), 2976–2980.

33. Namanja, H. A.; Emmert, D.; Hrycyna, C. A.; Chmielewski, J. Homodimers of the Antiviral Abacavir as Modulators of P-Glycoprotein Transport in Cell Culture: Probing Tether Length. *MedChemComm* **2013**, *4* (10), 1344–1349.

34. Emmert, D. ; Campos, C. R.; Ward, D.; Lu, P.; Namanja, H. A.; Bohn, K.; Miller, D. S.; Sharom, F. J.; Chmielewski, J.; Hrycyna, C. A. Reversible Dimers of the Atypical Antipsychotic Quetiapine Inhibit P-Glycoprotein-Mediated Efflux in Vitro with Increased Binding Affinity and in Situ at the Blood-Brain Barrier. *ACS Chem. Neurosci.* **2014**, *5* (4), 305–317.

35. Bohn, K.; Lange, A.; Chmielewski, J.; Hrycyna, C. A. Dual Modulation of Human P-Glycoprotein and ABCG2 with Prodrug Dimers of the Atypical Antipsychotic Agent Paliperidone in a Model of the Blood-Brain Barrier. *Mol. Pharm.,* **2017**, *14* (4) 1107–1119.

36. Namanja-Magliano, H. A.; Bohn, K.; Agrawal, N.; Willoughby, M. E.; Hrycyna, C. A.; Chmielewski, J. Dual Inhibitors of the Human Blood-Brain Barrier Drug Efflux Transporters P-Glycoprotein and ABCG2 Based on the Antiviral Azidothymidine. *Bioorg. Med. Chem.* **2017**, *25* (19), 5128–5132.

37. Schuster, I. I. A Carbon-13 NMR Study of Electronic Effects in the Hydrogen Bonding of Trifluoroacetic Acid with Substituted Benzenes, 1- and 2-Substituted Naphthalenes, and 9-Substituted Anthracenes in Chloroform. *J. Org. Chem.* **1985**, *50* (10), 1656–1662.

38. Hrycyna, C. A.; Ramachandra, M.; Pastan, I.; Gottesman, M. M. Functional Expression of Human P-Glycoprotein from Plasmids Using Vaccinia Virus-Bacteriophage T7 RNA Polymerase System. *Methods Enzymol.* **1998**, *292*, 456–473.

39. Namanja, H. A. Development of Dimeric Prodrug Inhibitors of P-glycoprotein and ABCG2 to Enhance Brain Penetration of Antiretroviral Agents. Ph.D. Dissertation, Purdue University, **2012.**

40. Lee, C. G.; Pastan, I.; Gottesman, M. M. Retroviral Transfer of Human MDR1 Gene into Human T Lymphocytes. *Methods Enzymol.* **1998**, *292*, 557–572.

41. Weksler, B. B.; Subileau, E. A.; Perrière, N.; Charneau, P.; Holloway, K.; Leveque, M.; Tricoire-Leignel, H.; Nicotra, A.; Bourdoulous, S.; Turowski, P.; Male, D. K.; Roux, F.; Greenwood, J.; Romero, I. A.; Couraud, P. O. Blood-Brain Barrier-Specific Properties of a Human Adult Brain Endothelial Cell Line. *FASEB J.* **2005**, *19* (13), 1872–1874.

42. Carl, S. M.; Lindley, D. J.; Das, D.; Couraud, P. O.; Weksler, B. B.; Romero, I.; Mowery, S. A.; Knipp, G. T. ABC and SLC Transporter Expression and Proton Oligopeptide Transporter (POT) Mediated Permeation across the Human Blood--Brain Barrier Cell Line, HCMEC/D3. *Mol. Pharm.* **2010**, *7* (4), 1057–1068.

43. Poller, B.; Gutmann, H.; Krähenbühl, S.; Weksler, B.; Romero, I; Couraud, P.-O.; Tuffin, G.; Drewe, J.; Huwyler, J. The Human Brain Endothelial Cell Line HCMEC/D3 as a Human Blood-Brain Barrier Model for Drug Transport Studies. *J. Neurochem.* **2008**, *107* (5), 1358–1368.

44. Mosmann, T. Rapid Colorimetric Assay for Cellular Growth and Survival: Application to Proliferation and Cytotoxicity Assays. *J. Immunol. Methods* **1983**, *65* (1–2), 55–63.

45. Richman, D. D.; Kornbluth, R. S.; Carson, D. A. Failure of Dideoxynucleosides to Inhibit Human Immunodeficiency Virus Replication in Cultured Human Macrophages. *J. Exp. Med.* **1987**, *166* (4), 1144–1149.

46. Davis, D. A.; Brown, C. A.; Singer, K. E.; Wang, V.; Kaufman, J.; Stahl, S. J.; Wingfield, P.; Maeda, K.; Harada, S.; Yoshimura, K.; Kosalaraksa, P.; Mitsuya, H.; Yarchoan, R. Inhibition of HIV-1 Replication by a Peptide Dimerization Inhibitor of HIV-1 Protease. *Antiviral Res.* **2006**, *72* (2), 89–99.

47. Tang, M. W.; Shafer, R. W. HIV-1 Antiretroviral Resistance: Scientific Principles and Clinical Applications. *Drugs* **2012**, *72* (9), e1-e25.

48. Pokorná, J.; Machala, L.; Řezáčová, P.; Konvalinka, J. Current and Novel Inhibitors of HIV Protease. *Viruses* **2009**, *1* (3), 1209–1239.

SYNOPSIS TOC

Heterodimers of HIV protease and reverse transcriptase inhibitors linked via a traceless tether are potent inhibitors of cellular P-gp efflux, and, in a reducing environment, revert to a monomeric combination therapy with *in cyto* anti-HIV-1 activity.

Insert Table of Contents artwork here